AUTOMATIC REGISTRATION FOR REPEAT-TRACK INSAR DATA PROCESSING

Mingsheng LIAO, Li ZHANG, Zuxun ZHANG, Jiangqing ZHANG
Wuhan Technical University of Surveying and Mapping,
Natinal Lab. for Information Eng. in Surveying, Mapping and Remote Sensing
Luoyu Road 129, Wuhan 430079, P. R. China
liao@wtusm.edu.cn

Working Group IC-1

KEY WORDS: InSAR, Registration, SAR processing, Automatic algorithm, Remote Sensing.

ABSTRACT

Interferometric Synthetic Aperture Radar (InSAR) allows production of high resolution DEM and detection of small earth motions using multiple pass SAR data sets obtained by remote sensing satellite. But the digital processing to extract the DEM is quite complicated. The whole procedure has not yet reached sufficient efficiency and robustness to warrant automated DEM production as commonly produced by stereo vision with optical images. The automatic algorithm for precision registration is one of the bottlenecks for improving both the accuracy and the efficiency of multi-source data analysis, including the repeat-track D-InSAR processing. In this paper, an automatic approach with multi-step image matching algorithm is presented. All procedures could be automatically implemented. The primary experiment result is promising in the fast precision registration for the repeat-track InSAR data and reveals the potential of the presented automatic strategy.

1 INTRODUCTION

InSAR presents a completely new approach for topographic mapping. But the whole process has not yet reached sufficient robustness to warrant automated DEM production as commonly produced by stereo vision with optical image (Trouve 1998). Moreover, the computing time should be kept as short as possible for an operative data processing system. One of the critical factors in generating the interferograms is the efficient and precise registration of the single look complex data. To obtain a high quality interference fringe pattern, it is necessary for the images to be registered to sub-pixel accuracy (Gabriel 1988, Zebker 1986).

Usually image registration deals with geometrical transformation and resampling of the pixel values. The identical points on both images can be identified as the control points. If sufficient control point pairs are determined, the transformation function could be chosen. The new pixel values are calculated according to the geometric transformation and the resample formulae (bi-linear or bi-cubic interpolation). The determination of suitable control point pairs has become the critical point.

The traditional method for registration usually utilizes the tie points which are manually determined. However, the manual procedure constitutes a tedious and time-consuming task and may be impossible for SLC SAR data. Various researchers have investigated the automatic matching approach (Zhang 1998). But it is much more difficult in SAR image matching than in traditional optical image since the speckle and the blur texture feature.

Lin *et al* presented the registration algorithm based on the optimization of a target with the average fluctuation function of the phase difference image (Lin 1992). Gabriel *ea tl* presented an approach based on the coherence estimation, which was adopted by many investigators (Gabriel 1988). A two-dimensional fast Fourier transform was performed on the interference fringe generated in the matching window, then the relative quality was assessed with the signal-noise ratio of the fringe spectrum. Zebker *et al* also used small patches as tie points on ERS images and performed the 2D convolutions to find maximum power spectra. Offsets in range and azimuth can be determined based on the difference of these patches (Zebker 1994). But in fact, the power distribution will differ greatly from the ideal case with a single peak. Multiple peaks may appear, resulting in difficulty in correlation determination (Wang 1990). In these algorithms, the generation of the fringe and the FFT are the very time consuming task. Additionally the entire matching procedure is repeated as the search area was scanned pixel by pixel.

In this paper, a multi-step matching approach based on intensity or power detected images is presented. In the primary matching, the distinct points are selected and their conjugation points are determined automatically based on the

✧ This research was funded by National Nature Science Foundation of China (Contract No. 69782001) and R&D Foundation for Surveying and Mapping Technology (Contract No.99008).

normalized correlation coefficient algorithm, which tolerates any linear radiometric relationship between the images. Then the global matching procedure based on the bridge mode and probability relaxation technique is used to ensure the reliability of the matching result. The automatic strategy has been used for the registration between SPOT and TM images, which are acquired from different sensors (Zhang 1998). Finally, the Least Square (LS) matching algorithm is used to improve the precision (less than 1/10 pix.). The frequency independent coherence estimator (Guarnieri 1997) is used as the matching criteria of LS algorithm. The experiment is carried out successfully with SIR-C / L&C band data.

2 METHODOLOGY

2.1 Primary Image Matching

The image matching is based on the measurement of similarity of image structures or gray level distribution between two images. At this scenario, only the intensity image of SLC data is used in image matching procedure. Firstly the feature points are detected with Forstner interest operator in the master image (Wang 1990), then the initial matching based on the similarity is conducted to find the candidates of the corresponding point in the slave image. The primary matching procedure employed normalized correlation coefficients between 0 and 1, which is defined as

$$\rho = \frac{C(p,q)}{\sqrt{C_{gg}(p,q)C_{g'g'}(p,q)}} \tag{1}$$

Here $C_{gg}(p, q)$ and $C_{g'g'}(p, q)$ are respectively the variance of master image $g(x, y)$ and slave image $g'(x, y)$, $C(p,q)$ is the covariance of $g(x, y)$ and $g'(x, y)$. The closer to 1 the value of ρ, the more similar images are to each other. The advantage of using the normalized correlation coefficient is that it tolerates any linear radiometric relationship between the two images. The computational complexity is not obvious.

But the single point matching does not take the compatibility of matching results with its neighbors into consideration. It is difficult to improve the reliability for only the finite information contained in a matching window. In order to overcome the drawback, an algorithm of global matching with relaxation has been developed and further used to the second step of our registration procedure, which ensure the reliability of the matching result (Zhang 1990).

2.2 Global Image Matching with Probability Relaxation

As well known, image matching is used to define the corresponding point pair, that is the point j in slave image corresponding to the point i in the master image. Assume that there are an object set $O=\{O_1, O_2, \ldots, O_n\}$ and a class set $C=\{C_1, C_2, \ldots, C_m\}$, the point i as an "object", the points j in slave image are classified into "class". If image matching is going to solve the problem of $O_i \in C_j$, the global consistency should be considered. Therefore the probability of $O_i \in C_j$ and the compatible coefficient $C(i,j; h,k)$ of $O_i \in C_j \cap O_h \in C_k$ must be defined according to the probability relaxation algorithm.

Since the area based matching algorithms use the similarity of gray level distribution as their measurement of image matching, the correlation coefficient ρ_{ij} may be used as the measurement of P_{ij} of $O_i \in C_j$. Based on the principle of

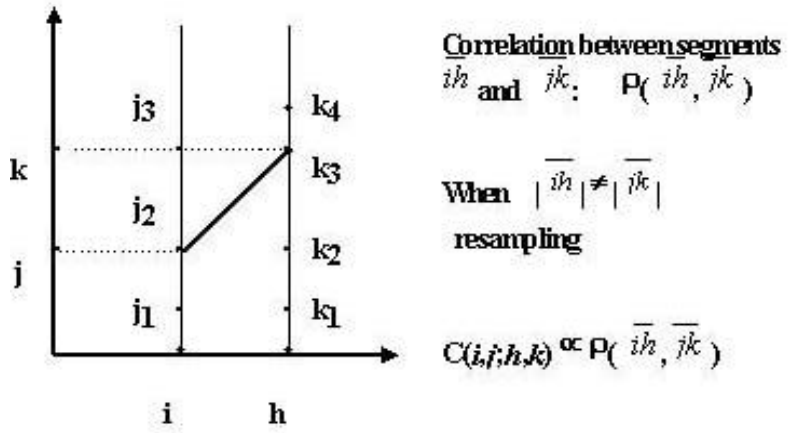

Figure 1. Probability relaxation with bridge model

bridge mode method as shown in Fig.1, the correlation coefficient $\rho(\overline{ih}, \overline{jk})$ between the image segment $\overline{ih}$ in the master image and the image segment $\overline{jk}$ in the slave image can be used as a measurement of the compatible coefficient $C(i,j;h,k)$ of $O_i \in C_j \cap O_h \in C_k$, i.e.:

$$C(i,j;h,k) \propto \rho(\overline{ih}, \overline{jk}) \tag{2}$$

After P_{ij} and $C(i,j;h,k)$ are defined, the relaxation iterative procedure would be induced,

$$\begin{cases} Q(i,j) = \sum_{h=1}^{n(H)} (\sum_{k=1}^{m(K)} C(i,j;h,k) \cdot P(i,j)) \\ P^{(r)}(i,j) = P^{(r-1)}(i,j) \cdot (1 + B \cdot Q(i,j)) \\ P^{(r)}(i,j) = P^{(r)}(i,j) / \sum_{j=0}^{m(J)} P^{(r)}(i,j) \end{cases} \tag{3}$$

Here n(H) is the number of neighbor points (8- or 24-neighbourhood), m(K) and m(J) is the number of the candidates. The scalar B is a constant with which the convergence rate of the iteration procedure could be adjusted. The value $P(r)$ determines whether the iteration is stop. Finally the reliable point pair can be confirmed if $P^{(r)} > T$, here T is the threshold.

2.3 LS Matching Procedure

The relaxation algorithm discussed above can improve the reliability of the determination of the conjugate point. But it is difficult to refine the matching accuracy. It is necessary to take the further procedures. As well-known, LS correlation method has successfully been developed, which could achieve very high accuracy of correlation by means of minimization of the root mean square value of the gray value differences of the image pair. Here the principle of minimization of grey value differences between the two correlation windows is used instead of the conventional approach based on maximization of the correlation coefficient (Rosenholm 1986).

We describe the general principle in one-dimensional case. Assume that there are two grey value functions $g_1(x)$ and $g_2(x)$ with an image pair. In an ideal case, these two functions should be the same except for a displacement x_0 between them. Their noises are $n_1(x)$ and $n_2(x)$ respectively. Then the observation functions are shown as (subscript i representing the corresponding values at pixel i):

$$\begin{cases} \overline{g}_1(x_i) = g_1(x_i) + n_1(x_i) \\ \overline{g}_2(x_i) = g_2(x_i) + n_2(x_i) = g_1(x_i - x_0) + n_2(x_i) \end{cases} \tag{4}$$

$$\Delta g(x_i) = \overline{g}_2(x_i) - \overline{g}_1(x_i) = g_1(x_i - x_0) - \overline{g}_1(x_i) + n_2(x_i) - n_1(x_i) \tag{5}$$

Assume x_0 to be small, we linearize $g_1(x_i - x_0)$ in the 1st order term and write equation(5) again as following:

$$\Delta g(x_i) + v(x_i) = -\dot{g}_1(x_i) \cdot x_0 \tag{6}$$

where $v(x_i) = n_1(x_i) - n_2(x_2)$, which is the linearized error equation. The observed value is the gray value difference $\Delta g(x_i)$. The unknown value is x_0. Using the method of Least Squares, the following equation is obtained and value x_0 is thus solved:

$$\sum v^2(x_i) = \sum (n_1(x_i) - n_2(x_i))^2 = \min \tag{7}$$

Practically, since each pixel pair can constitute an error equation, there are M×M observed values within a M×M matching window, which are redundant for the solution of x_0. Because the linearization exists in Equation (6), the solution has to be iterated.

The principle can be easily generated into 2D image matching case. Herewith the initial values for the iteration can be obtained from the result of the relaxation matching as described in Section 2.2. Theoretically the accuracy of determination for conjugate points in this method may reach the order of 1/50 to 1/100 pixel. Considering other factors, the accuracy of 1/10 pixel for InSAR data registration will be satisfactory.

2.4 The Criteria for LS Matching Iterative Procedure

Since the LS matching is an iterative procedure, the criteria for the matching should be selected to decide whether the iterative is stopped. Herewith the correlation coefficient of the SLC images is used as the criteria, which is usually adopted as the coherence measurement of fringe. The correlation coefficient is calculated according to

$$\gamma = \frac{|E[u_1 u_2^*]|}{\sqrt{E[|u_1|^2]E[|u_2|^2]}} \tag{8}$$

Its estimation holds

$$\bar{\gamma} = \frac{\left| \sum_{n=0}^{N} \sum_{m=0}^{M} u_1(n,m) u_2^*(n,m) e^{-j\varphi(n,m)} \right|}{\sqrt{\sum_{n=0}^{N} \sum_{m=0}^{M} |u_1(n,m)|^2 \sum_{n=0}^{N} \sum_{m=0}^{M} |u_2(n,m)|^2}} \tag{9}$$

where u_1, u_2 are the SLC images to be registered, N×M is the size of the estimation window.
But it should be noted that even if the ergodicity hypothesis holds, the accurate interferometric phase should be estimated and compensated in expression (9). The complexity is highly increased. Therefore the frequency independent estimator is introduced. So the absolute value of the complex coherence can be calculated as

$$\bar{\gamma}_M = \begin{cases} \sqrt{2\bar{\rho} - 1} & \bar{\rho} > 0.5 \\ 0 & \bar{\rho} \le 0.5 \end{cases} \tag{10}$$

where

$$\bar{\rho} = \frac{\sum_{n=0}^{N} \sum_{m=0}^{M} |u_1(n,m)|^2 |u_2(n,m)|^2}{\sqrt{\sum_{n=0}^{N} \sum_{m=0}^{M} |u_1(n,m)|^4 \sum_{n=0}^{N} \sum_{m=0}^{M} |u_2(n,m)|^4}} \tag{11}$$

The estimator described in expression (10) and (11) is much more efficient in computational costs than the usual estimator, despite a reduced statistical confidence. If the coherence is not very low and the estimation window is large, the accuracy will be good enough as the matching criteria (Guarnieri 1997).

3 EXPERIMENTS

The multi-step matching method is applied on the registration between an SLC image pair of SIC-C/C&L-band. All the procedures were implemented automatically. The images cover the Hawaii area as shown partly in Fig.2. The portion with image size 2500×2500 is used as the test site. The image pair of L-band is shown in Figure 2.

More than 100 point pairs have been determined within a short period of time with about 0.5 to 1 pixel RMS by global relaxation algorithm. The cross cursors marked in Fig.2 indicate the conjugate point pairs. Then the point pairs were input as the initial values for the Least Square Matching. After about 5 LS iterations, the RMS of the global polynomial transformation is less than 1/10 pixel. The Table 1 and Table 2 show the results from L-band image pair and C-band image pair respectively. The window size for matching and coherence estimation is 63×63. So some points were cancelled because they were very close the image edge. The geometric registration was performed by means of 2'nd order polynomials. The accuracy after LS matching is less than 1/10 pixel and available for InSAR data processing. Finally the fringes and coherence images were multi-look processed with 2 looks in range and 2 looks in azimuth. The fringes and coherence images are shown in Figure 3 and Figure 4 respectively. About 7 minutes was required for one image pair with image size 2500×2500 on Indigo-2 workstation. The program code will be optimized further.

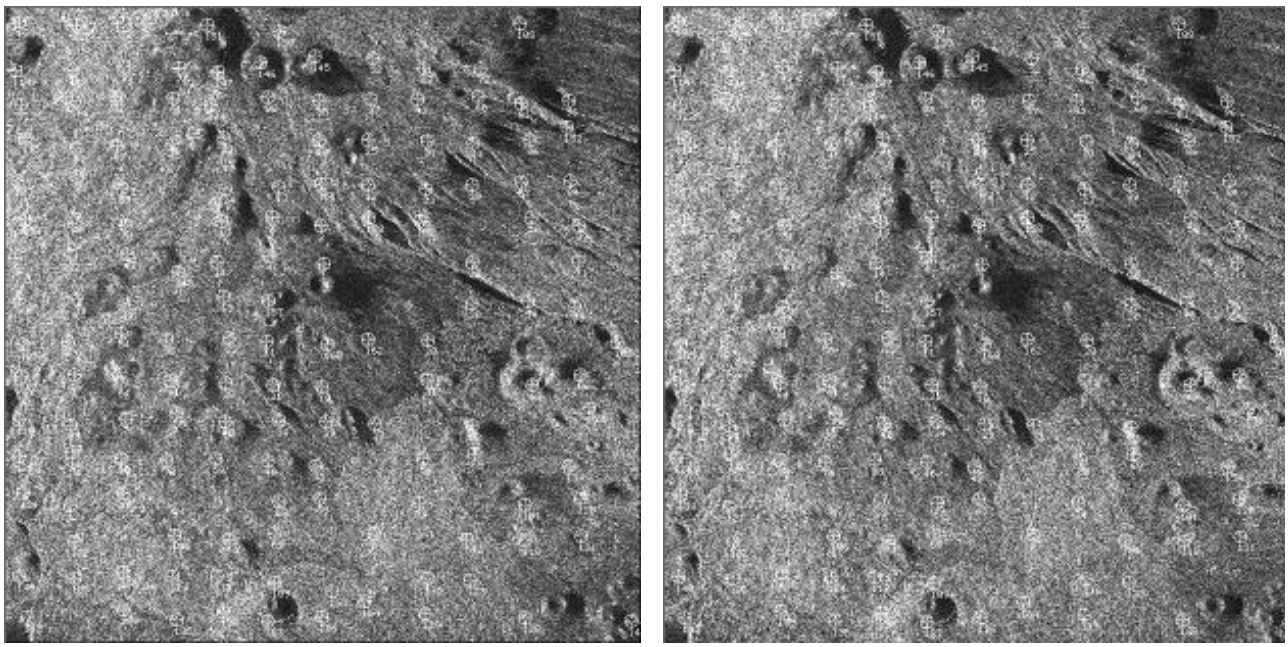

Figure 2. The L-band image pair

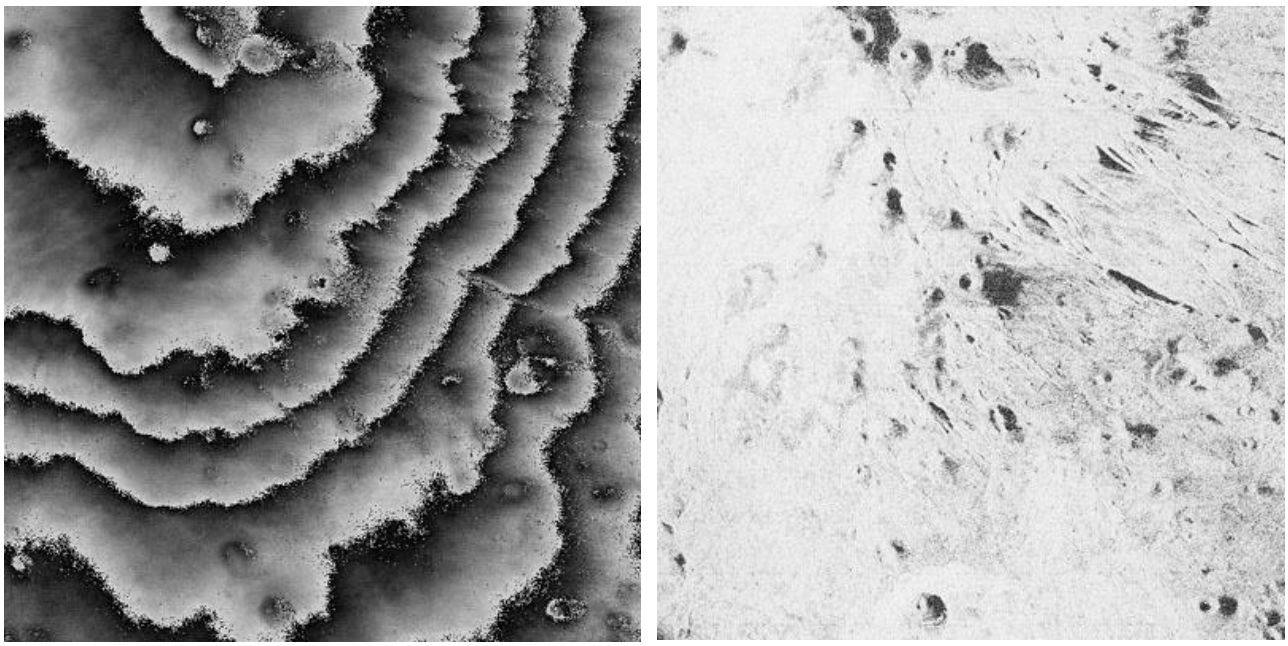

Figure 3.

(a) Fringe from the L-band image pair (b) Coherence image from the L-band image pair

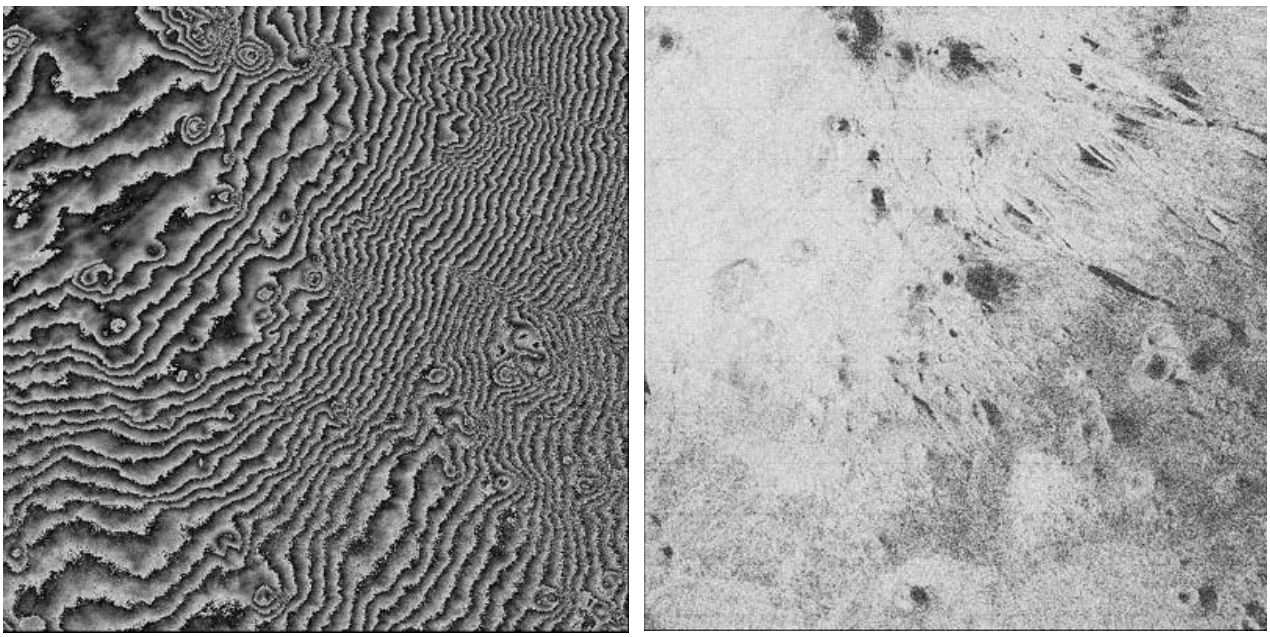

Figure 4.

(a) Fringe from the C-band image pair (b) Coherence image from the C-band image pair

Matching algorithm	RMS Error				Maximum residual		
	Number of Points	Range	Azimuth	Total RMS	Range	Azimuth	Total residual
Only relaxation matching	155	0.160	0.123	0.201	1.980	0.447	1.985
Least Square Matching	152	0.065	0.026	0.063	0.768	0.140	0.781

Table 1. L-band image pair: the comparison of the accuracy with different method

Matching algorithm	RMS Error				Maximum residual		
	Number of Points	Range	Azimuth	Total RMS	Range	Azimuth	Total residual
Only relaxation matching	105	0.096	0.191	0.214	0.971	0.639	0.984
Least Square Matching	98	0.035	0.042	0.055	0.229	0.137	0.237

Table 2. C-band image pair: the comparison of the accuracy with different method

4 CONCLUSIONS

An efficiency registration approach for InSAR data processing based on multi-step matching is presented. The experiment result indicates its promising possibility in InSAR data processing. It appears to be a good compromise

between accuracy and computation cost. The procedures were implemented automatically. Further investigation will focus on the evaluation of the accuracy and reliability of the DEM quality generated in the next steps.

ACKNOWLEDGMENTS

The authors would like to thank Mr. Jie YANG, Wen YANG and Pan ZHU *et al* for the technical support.

REFERENCES

Gabriel, A. K., R. M. Goldstein, 1988. Crossed orbit interferometry: Theory and experimental results from SIR-B. Int. J. Remote Sensing, 9(5), pp. 857-872.

Guarnieri, M. A. and Claudio Prati, 1997. SAR Interferometry: A "Quick and Dirty" Coherence Estimator for Data Browing. IEEE Trans. On Geos.&RS., 35(3), pp.660-669.

Lin, Q., J. F. Vesecky, 1992. Registration of Interferometric SAR Images. Proceedings of IGARSS'92, pp. 1579-1581.

Rosenholm, D., 1986. Accuracy Improvement of Digital Matching for Evaluation of Digital Terrain Model, IAPRS, Vol. 26, Comm. III, Rovaniemi, pp.573-587.

Trouve, E., Nicolas J., and Maitre H., 1998. Improving Phase Unwapping Techniques by the Use of Local Frequency Estimates. IEEE Trans. On Geos.&RS., 36(6), pp.1963-1972.

Wang, Z., 1990, Principles of Photogrammetry (with Remote Sensing), Publishing House of Surveying and Mapping, Beijing

Zebker, H.S., Goldstein R. M., 1986. Topographic Mapping from Interferometric Synthetic Aperture Radar Observations. J. Geophys. Res., Vol.91(B5), pp.4993-4999.

Zebker, H. A., Werner C. L., Rosen P. A., Hensley S., 1994. Accuracy of Topographic Maps Derived from ERS-1 Interferometric Radar. IEEE Trans. on Geos.&RS., Vol.32, pp.823-835.

Zhang, Z. *et al*, 1990. Image Matching by Bridge Mode Based on Dynamic Programming. Int. Arch. Of ISPRS, *Vol.28, Part 3/2,* Wuhan, China, pp.1106-1120.

Zhang, Z., Zhang J., Liao M., Zhang L., 1998. Automatic registration between SPOT and TM images. Proceedings of SPIE, Vol.3545, pp.358-361